Experimental investigation of pressure characteristics in the duct flow with an inclined jet injection

—— Difference between the flowfield by full span and partial span injection ——

Akisato MIZUNO, Kogakuin University, Nakano-machi 2665, Hachioji, 192 Tokyo, Japan
Ryota YANO, Kogakuin University
Tohru YAMAZAKI, Kogakuin University

ABSTRACT

Experimental study is carried out to clarify the duct flow with an inclined jet injection, as the model test of tunnel ventilation facility. A 8,800mm long duct with 230mm x 230mm square cross section is constructed, and an injection nozzle with 20mm x 230mm outlet with the angle of 30° is installed at 2,100mm from the inlet. In addition to full span injection, the nozzle with 80% span is installed to observe the effect of three dimensionality. Measured pressure gains under various flow ratios showed good agreement with the theory based on the law of momentum. The velocity distribution with full span injection showed the existence of two dimensional separation bubble, while partial injection cases revealed a stronger down wash.

INTRODUCTION

Inclined jet injection is applied to longitudinal tunnel ventilation, in order to induce flow in the tunnel. Generally, the pressure rise effect of the ventilators, such as jet fans and large scale fans at the vertical shaft, is estimated by theoretical formulae induced by momentum theory[(1)(2)(3)(4)]. However, the pressure characteristics of the duct flow with an inclined jet, as well as the velocity field, is not yet known well, and a systematic study is considered to be necessary.

In the present paper the authors carry out a series of model experiment with a scale of 1/30, and the pressure gain performance is measured and compared with theory. The flowfield and the mixing process after the injection is also measured in detail to find out to which extent the high velocity air flow can affect the traffic in the actual tunnel. In the current experiment, the Reynolds number is smaller in comparison to the one in the actual phenomena, the authors consider that the intrinsic characteristics are common with the actual system.

NOMENCLATURE

A：Cross sectional area of the duct
A_j：Area of jet exhaust
C_p：Pressure coefficient
D：Hydraulic diameter
P：Pressure
Q_1：Flow rate in the upper stream
Q_2：Flow rate in the down stream
Q_j：Injection flow rate
Re：Reynolds number $=V_2D / \nu$
V_1：Mean velocity in the upper stream
V_2：Mean velocity in the down stream
V_j：Jet velocity
ΔC_p：Coefficient of pressure gain
κ：Flow ratio $=Q_j / Q_2$
ρ：Air density
ψ：Area ratio $=A_j / A$

EXPERIMENTAL APPARATUS

Fig. 1 shows the coordinate system of the apparatus, in which the main flow direction is *z*. A side view of the whole apparatus is illustrated in Fig. 2. The main duct has a cross section of 230mm x 230mm square (For a square, the side length is equal to hydraulic diameter, which is taken as the reference length) with a bell-mouth and honeycomb/mesh combination at the inlet. Total length of the experimental setup is 8,800mm with 7,700mm straight

duct, made of plexi-glass. The exhaust fan at the end of the duct is driven by an inverter to control the main flow to be in the range from 4.0 to 13 m/s. The Reynolds numbers correspond from 6.6×10^4 to 2.1×10^5 respectively. An inclined air jet is blown into the main duct at 2,100mm downstream from the inlet, with the angel of 30°, which is the case often used. The flow velocity of the jet can be set arbitrarily. The flow rate of the main duct is set to the prescribed value in terms of pressure difference of the inlet bellmouth, based on the calibration by measuring the flow rate as the integration of the velocity distribution.

The ratio of flow rates of jet injection and the main duct downstream is defined as κ, taking the range of 0 to 0.5, adding an extreme case of κ=1.0, where inlet flow to the main duct is closed. The authors prepared two nozzles in order to compare two- and three-dimensional injections. Both has a gap of 20mm and a width of 230mm for full span injection, which produces nearly two-dimensional flow, and of 184mm for partial injection (spanwise contraction to 80% of the original injection area), in which a strong three-dimensionality is expected.

THEORETICAL CONSIDERATION

The inflow and outflow momentum through the control surface shown in Fig. 3 are

$$M_{in} = \rho Q_1 V_1 + \rho Q_j V_j \cos\beta \quad (1)$$

$$M_{out} = \rho Q_2 V_2 \quad (2)$$

in which downstream surface is taken to be far from the injection. Hence, the pressure difference is given by momentum theory in the form

$$A(P_2 - P_1) = \rho Q_1 V_1 + \rho Q_j V_j \cos\beta - \rho Q_2 V_2 \quad (3)$$

where

$$V_1 = (Q_2 - Q_j)/A \quad (4)$$

$$V_2 = Q_2/A \quad (5)$$

By substituting Eqs. (4) and (5) into Eqs. (3), the pressure gain

$$\Delta P = 2\frac{Q_j}{Q_2}\left\{\frac{Q_j}{Q_2} + \frac{V_j \cos\beta}{V_2} - 2\right\}\frac{1}{2}\rho {V_2}^2 \quad (6)$$

is obtained. It is converted in terms of flow ratio κ and area ratio ψ to the expression,

Fig. 3 Application of momentum law

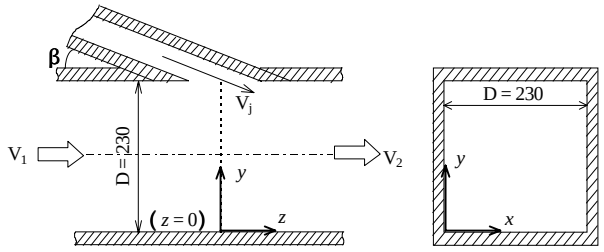

Fig. 1 Coordinate system

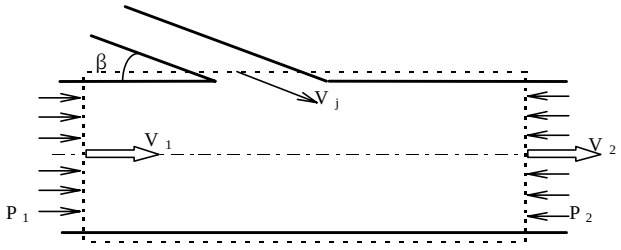

$$\Delta P = 2\kappa\left\{\kappa + \frac{\kappa}{\varphi}\cos\beta - 2\right\}\frac{1}{2}\rho {V_2}^2 \quad (7)$$

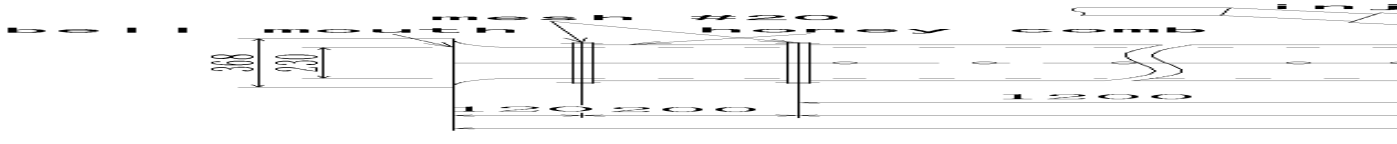

Fig. 2 Experimental apparatus

The non-dimensional pressure gain is therefore obtained by dividing Eq. (7) with the dynamic pressure based on the downstream mean velocity $\left(\rho V_2{}^2/2\right)$ as

$$\Delta C_p = 2\kappa\left\{\kappa + \frac{\kappa}{\varphi}\cos\beta - 2\right\}. \quad (8)$$

MEASUREMENT OF PRESSURE DISTRIBUTION

The pressure distribution along the *z*-axis is measured through the pressure holes every 100mm at the height of 115mm. The diameter of the hole is 1mm. One of the measured pressure distributions is shown in Fig. 4. The pressure decreases linearly from the beginning to the injection nozzle. After the injection (z=0), the pressure rises to be the highest value some 2m downstream, from which it again decreases linearly with a slightly larger inclination. For the convenience of the later processing, the pressure data are made non-dimensional by dividing by the dynamic pressure of the downstream velocity, which gives the pressure coefficient C_p.

The *z*-axis is divided by the reference length D(=230mm) to obtain the non-dimensional coordinate. Following cases are depicted in the non-dimensional form. Figure 5 shows the non-dimensional pressure distribution in the case of the largest κ(=0.512), in which a large pressure gain is attained. On the other hand, without injection, no pressure recovery is observed (κ=0: Fig. 6). In Fig. 7, the process of obtaining pressure gain is explained. Fitted lines at both sides of the injection are extrapolated to the coordinate z=0, and the pressure gain is given as the difference at the location as ΔC_p. In this process least square method is used and the data in the range from $-6D$ to $-0.4D$ and from 14D to 23D are used, where the data are well on straight lines with different inclinations for all the cases. The experimental pressure gains are compared with the theoretical ones in the later section.

Figures 8 through 10 are the results under partial injection, which does not show much difference with the former results.

VELOCITY DISTRIBUTION

Measurement of velocity distribution is carried out at the sections of 0.5D, 1D, 2D, 3D, 5D, 10D, 15D and 20D. At each section, there are five holes at x=0.1D, 0.3D, 0.5D, 0.7D and 0.9D, where a Pitot tube can be traversed in the *y*-direction. In the Figs. 11 through 13 the velocity distribution are shown in the case of ψ= 0.087 (full span injection), in which velocity is non-dimensionalized with the downstream mean velocity V_2. The mixing process of the injected flow is observed in the figures. The injected flow is in a high velocity and confined in the upper wall region, then loses the speed gradually by turbulent mixing, while it flows downstream. In the cases with larger ratio of flow rate, the velocity profile finally comes back to symmetry around 20D. However, in the case of the smallest flow ratio (κ =0.214), uniformity is not yet attained even at 20D.

Velocity vector is measured with a four-holed Pitot tube[5][6]. The velocity component in *y*-*z* plane in the central cross section (x=0.5D) is illustrated in Figs. 14 and 15. It is observed that at the beginning the jet flows in the injected direction, but turns back toward the upper wall, composing a separation bubble.

The velocity profiles for partial injection are shown in Figs. 16 and 17, in which the area ratio $\psi$is 0.070. By comparing the case of κ=0.280 (Fig. 16) with the counterpart with similar flow ratio (Fig. 11), it is noted that higher velocity region reaches closer to the bottom wall at cross section of z=2D to 5D, due to three-dimensionality. As the injection area is 80% of the span, it is less likely that a closed separation bubble is composed, which caused this tendency. In the lower flow ratio, it takes longer distance until a symmetrical velocity distribution is recovered, which is also the case for the full span injection.

COMPARISON OF THEORETICAL PRESSURE GAIN WITH EXPERIMENTAL RESULTS

Non-dimensional pressure gain vs. flow ratio is depicted in Figs. 18 and 19. Experimental results are plotted on the theoretical curve, and they agree well in both cases. The friction loss, observed in refs. (3) and (4), is not relevant in the current results, presumably because the inclined jet does not lose its momentum due to wall friction.

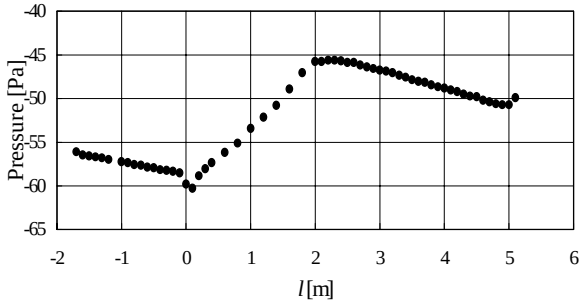

Fig. 4 Pressure distribution along the duct axis

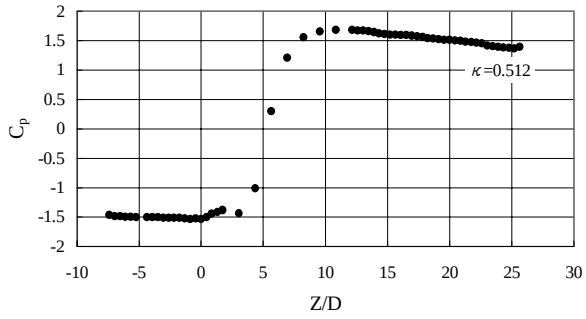

Fig. 5 Distribution of pressure coefficient
(full span κ=0.512)

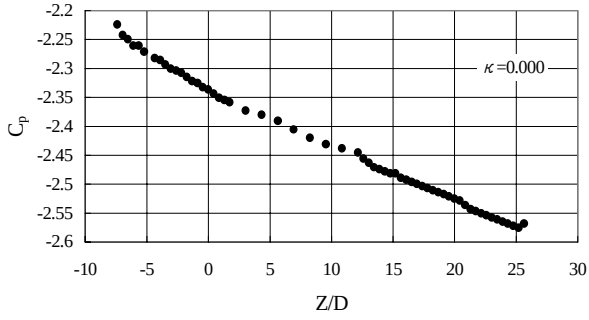

Fig. 6 Distribution of pressure coefficient
(full span κ=0.000)

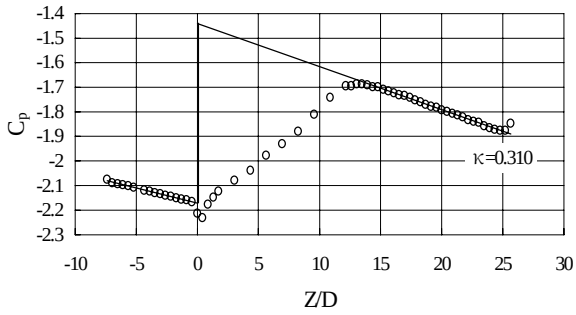

Fig. 7 Distribution of pressure coefficient
(full span κ=0.310)
(Explanation how to obtain pressure gain)

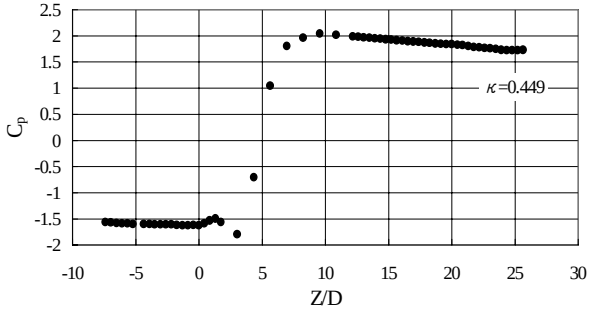

Fig. 8 Distribution of pressure coefficient
(partial span κ=0.449)

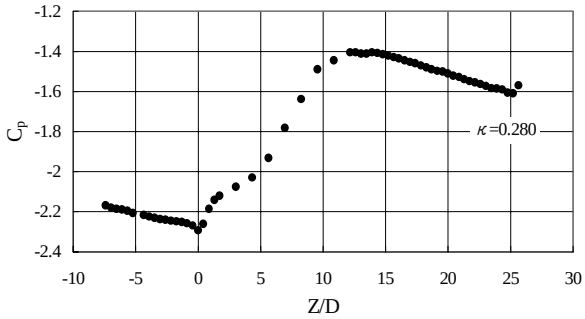

Fig. 9 Distribution of pressure coefficient
(partial span κ=0.280)

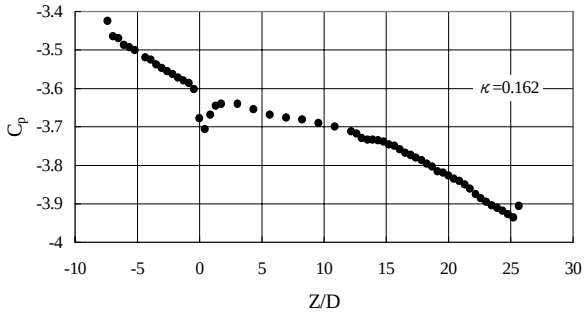

Fig. 10 Distribution of pressure coefficient
(partial span κ=0.162)

CONCLUSION

Experimental investigation was carried out of the pressure gain measurement of an inclined jet injection into a square duct under various flow ratios and other parameters. The pressure gains showed good agreement with the theoretical values. This is due to a smaller wall friction in comparison to the former works, where the injection was parallel to the wall.

Through measurements of the velocity distribution, the mixing process of the jet is made clear. In the cases with lower flow ratio, it took a longer distance until the velocity distribution is recovered. The reason is not clear, but it can be imagined that when the jet speed is similar to the main stream, the distortion of the velocity distribution can be easily transferred with less relaxation effect.

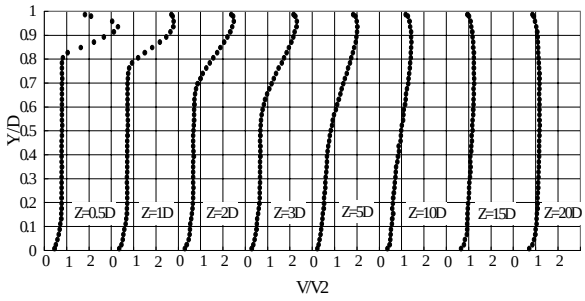

Fig. 11 Velocity distribution (full span κ =0.310)

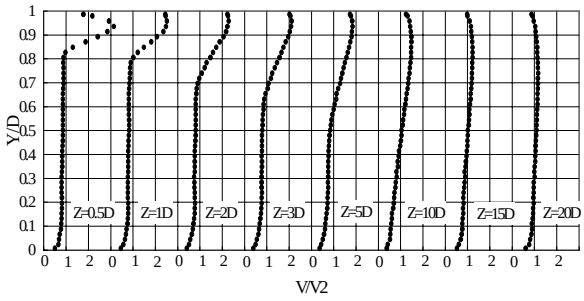

Fig. 12 Velocity distribution (full span κ =0.251)

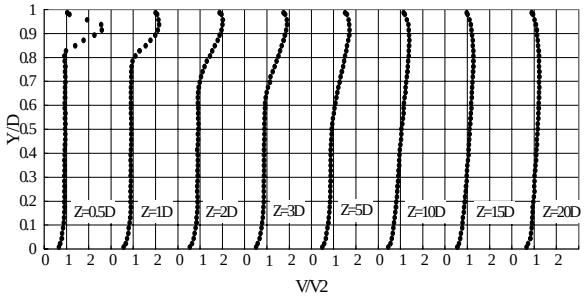

Fig. 13 Velocity distribution (full span κ =0.214)

By injecting from the nozzle with 80% span of the duct, the velocity distribution spread to the area father from the ceiling than the one with full span injection. This is obviously due to being three dimensional flow, and a high velocity region spreads downward. Although the experiment was carried out at a lower Reynolds number than the actual one, which may lead to quantitative discrepancy, the results obtained in the current study is considered to hold also in the actual scale.

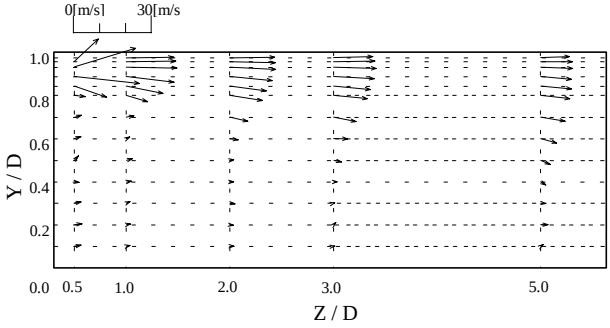

Fig. 14 Velocity vectors (full span κ =0.512)

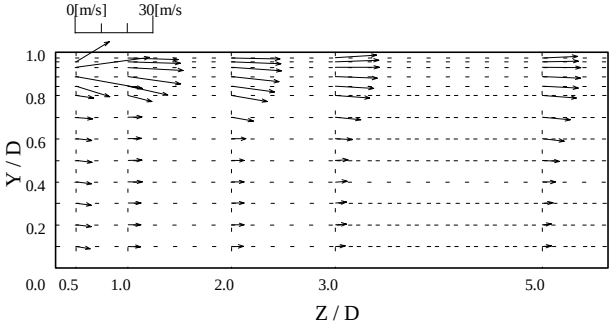

Fig. 15 Velocity vectors (full span κ =0.310)

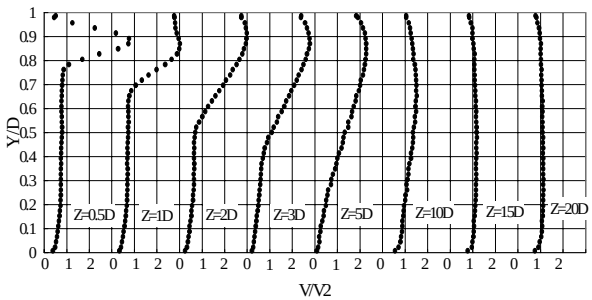

Fig. 16 Velocity distribution (partial span κ =0.280)

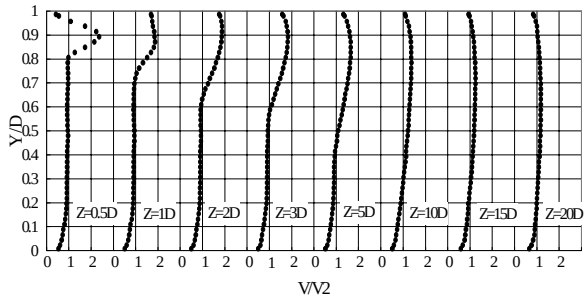

Fig.17 Velocity distribution (partial span κ =0.162)

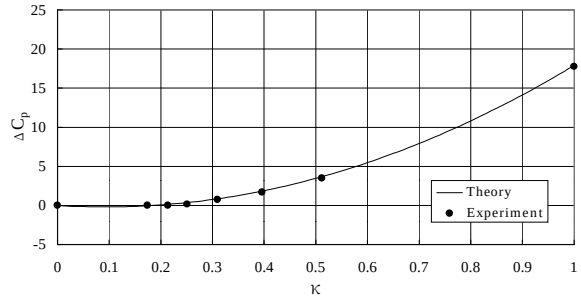

Fig. 18 Coefficient of pressure gain
(full span injection)

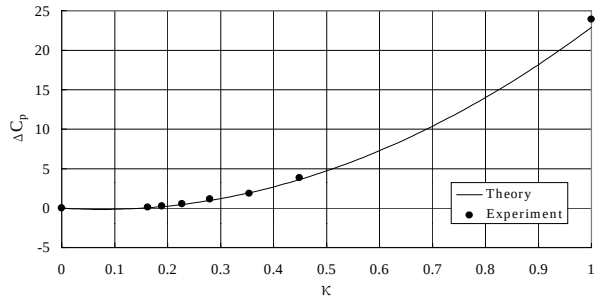

Fig.19 Coefficient of pressure gain
(partial injection)

REFERENCES

(1) Japan Road Association(ed.)., Technical guideline of road tunnels (ventilation), (in Japanese), Maruzen Co., (1985).

(2) Technology Center of Metropolitan Expressway., Report on Survey and Research on Tunnel Ventilation Design Principles, Metropolitan Expressway Public Corporation (1993).

(3) Mizuno, A. and Araie, K., Measurement of Pressure Rise Performance of a Jet Fan in a Tunnel by Model Experiment, Trans. Jpn. Soc. Mech. Eng., (in Japanese), Vol. 55, No. 514, B (1988), pp. 1613-1617.

(4) Mizuno, A. Araie, K. and Osato, H., Pressure Rise Effect by an Electrostatic Precipitator Station at Tunnel Crown, Trans. Jpn. Soc. Mech. Eng., (in Japanese), Vol. 56, No. 530, B (1989), pp. 3012-3017.

(5) Mizuno, A. and Morioka, T., Three-dimensional velocity vector measurement by five-holed Pitot tube with holes selection method, The 6th Asian Congress of Fluid Mechanics, May 22-26, 1995, Singapore, pp. 1062-1065

(6) Mizuno, A. and Morioka, T., Three-dimensional automatic velocity vector measurement by four-holed Pitot tube, Turbomachinery (in Japanese), Vol. 24, No. 12, (1996), pp. 725-731.